# Modelling Evolution of Directional Spectra of Water Waves (Workshop on Nonlinear Water Waves)

AUTHOR(S):

Annenkov, S. Y.; Shrira, Victor I.

CITATION:

Annenkov, S. Y. ...[et al]. Modelling Evolution of Directional Spectra of Water Waves (Workshop on Nonlinear Water Waves). 数理解析研究所講究録 2019, 2109: 100-114

ISSUE DATE:

2019-04

URL:

http://hdl.handle.net/2433/251947

数理解析研究所講究録 第2109巻 2019年 100-114



# Modelling Evolution of Directional Spectra of Water Waves

S.Y. Annenkov and V.I. Shrira
Keele University, UK

**Abstract**

Studies of the evolution of water wave spectra are usually focussed on frequency or wavenumber spectra of energy or wave action. Much less is known about the shape, or even width of the angular distribution and its evolution with time or fetch. Here, we consider the evolution of angular width of wave spectra with and without wind forcing. As a metric of the angular width, we use the second moment of the distribution at certain wavenumbers relative to the wavenumber of the spectral peak $k_p$ (0.5, 1, 2 and $3k_p$), or averaged over all wavenumbers. Numerical experiments are performed using three different numerical approaches employing different sets of assumptions: the classic Hasselmann kinetic equation (KE), the generalized kinetic equation (gKE) and the direct numerical simulation (DNS) algorithm based on the Zakharov equation (DNS-ZE). The results of simulations by each model are compared with each other and with the Tehuantepec field observations by Romero & Melville (2010). For the case of initially narrow swell the kinetic equations considerably overestimate the rate of the initial angular broadening , compared with the DNS-ZE, although at large time the integrated angular width approaches the same powerlike asymptote. The angular width of the spectral peak continues to grow slowly even for large time. For constant wind forcing, the models agree well on the spectral width of the spectral tail, but show large discrepancies for small wavenumbers. The DNS-ZE simulations are more consistent with the data of the Tehuantepec observations, demonstrating slow growth of angular width over time at the spectral peak, in contrast to nearly constant width shown by the kinetic equations. Results of the study demonstrate serious shortcomings of modelling based on the Hasselmann kinetic equation and provide an insight into the role of the assumptions underlying the Hasselmann equation.

## 1 Introduction

Studies of oceanic wind waves are mostly concerned with the evolution of wave spectra, mostly of one dimensional (frequency or wavenumber) spectra of energy or wave action. Spatio-temporal evolution of directional characteristics is less known. Observations of the spatio-temporal evolution of directional spectra are very difficult and, therefore, rare; they require precise measurements of two-dimensional spectra with a good angular resolution over a sequence of fetches. Parameterizations of wind wave spectra usually involve a representation of the directional distribution in the form $D(\theta)$, where $\theta$ is the angle, while the dependence of the function $D$ on

frequency or wavenumber is often ignored (Holthuisen, 2007). Even in this idealised case, the shape of the function $D(\theta)$ is not well known, usually it is assumed it having a maximum in the downwind direction (for which it is convenient to set $\theta = 0$) and a gradual decrease with increasing absolute value of $\theta$. Several expressions to describe this scale averaged behaviour of $D(\theta)$ have been proposed (e.g. $\cos^2$ model, $\cos^N$ model, the wrapped-normal distribution, etc). On summarising a large number of observations (Young *et al.*, 1995; Ewans, 1998) concluded that the directional width also varies with frequency, increasing approximately two-fold between $\omega_p$ and $3\omega_p$, where $\omega_p$ is the frequency of the spectral peak. To take into account the frequency dependence of $D(\theta)$ Mitsuyasu *et al.* (1975) suggested a piecewise-constant function, with the directional spreading being narrowest around the spectral peak frequency and widening towards both lower and higher frequencies. The value of the function at the spectral peak was also related to wind speed. There were further attempts at improvement the piecewise-constant relationship Goda (2010). Donelan et al (1985) suggested to use $\mathrm{sech}^2(\beta\theta)$, where $\beta$ is a piecewise-constant function of frequency $\omega/\omega_p$, independent of wind speed. Little is known about the evolution of $D(\theta)$ with fetch or time.

Numerical simulations of long-term spectral evolution also often focus on the evolution of one-dimensional (frequency or wavenumber)spectra. Badulin & Zakharov (2017) performed extensive simulations of swell evolution with the Hasselmann kinetic equation (KE). They have found that regardless of the initial angular width there is a tendency to a universal directional distribution at large times, which appeared to be quasi-stationary at least at the frequency corresponding to the spectral peak.

Until very recently, all numerical studies of long-term evolution of random water wave fields were based on the KE. The KE is based on two key assumptions: the statistical closure, occuring as a result of an asymptotic procedure based on small nonlinearity for broadband wave fields under the presumed absence of coherent patterns, and the quasistationarity implied by the large-time limit (Annenkov & Shrira, 2006*a*; Newell & Rumpf, 2013). To describe situations with a rapid transformation of a wave field, Annenkov & Shrira (2006*a*) derived a generalization of the KE called the generalized kinetic equation (gKE). The gKE employs the same statistical closure, but is free from the quasistationarity assumption. However, the role and validity of the statistical closure can be verified only by direct numerical simulation (DNS). Until recently, progress in clarifying this issue was very slow, since there were no tools for studying the long-term evolution of wave spectra without a statistical closure. Although there were a few attempts at modelling the spectral evolution with DNS, starting with Tanaka (2001), the algorithms used were very demanding in computational resources and, therefore, able to trace only the initial part of the evolution. The DNS algorithm, based on the Zakharov equation (DNS-ZE), was first suggested and implemented by Annenkov and Shrira (2001) for simulations of deterministic evolution of wave field, then modified and extended for modelling random wave fields in Annenkov & Shrira (2009), it was later used for the study of the spectral evolution under gusty wind (Annenkov & Shrira, 2011) and for simulations of the evolution of higher statistical moments of wave field (Annenkov & Shrira, 2013; Shrira & Annenkov, 2013). The algorithm is based on integration of the deterministic four-wave Zakharov equation and ensemble averaging over a sufficient number of realisations, and is free from any statistical assumptions.

Annenkov & Shrira (2018) examined the evolution of initially narrow (in both frequency and

angle) spectra subjected only to dissipation localised at high frequencies, using all three numerical models: the KE (the standard WRT algorithm was kindly provided by G. van Vledder), the gKE and the DNS-ZE. The reason for this particular choice of the initial conditions was the vast amount of observational and numerical data relevant to these spectra. In particular, they were used in the MARINTEK wave tank experiments described by Onorato *et al.* (2009) and Toffoli *et al.* (2010), so that detailed observations of the initial stages of both the spectral evolution and the evolution of higher statistical moments were available. Since these spectra were initially far from equilibrium, at the initial stage of evolution they undergo relatively fast broadening. Annenkov & Shrira (2018) found a striking difference in the rate of this angular broadening, which was much larger for the gKE and the KE than for the DNS-ZE. At the same time, results of the DNS-ZE simulations were consistent with earlier short-term DNS simulations by Xiao *et al.* (2013) carried out with the well-established high-order spectral method, the striking discrepancy between the kinetic equations and DNS could have been reported earlier, but apparently was not noticed. However, since the focus of Annenkov & Shrira (2018) was on the detailed comparison of frequency spectra, all computations were performed within the same, relatively narrow, angular sector $-4\pi/9 \le \theta \le 4\pi/9$, which could have affected the long term evolution of angular spread. In particular, the WRT code employed for the KE simulations proved to be sensitive to the choice of the angular segment, especially for simulations of angular spreading.

In this paper, we consider the long-term evolution of directional width of water wave spectra with and without wind forcing. The aim is to compare evolution of directional spectra obtained with different models, in order to reveal the role of different sets of assumptions under different winds. As a metric of directional width, we use the second moment of directional distribution, either at particular wavenumbers relative to the spectral peak $k_p$, or integrated over a wide range of wavenumbers.

First, we revisit the evolution of initially narrow spectra without wind, considered by Annenkov & Shrira (2018). For the present study, the KE simulations of evolution have been rerun for larger time and in the full circle rather than in a sector. At relatively short times, both KE and gKE show close evolution of directional width. However, the DNS-ZE simulations predict much slower rate of directional spreading of the spectral tail. In the long term, all models appear to tend to the powerlike spreading of approximately the same rate, although the DNS spectra have considerably larger directional width of the spectral peak.

Second, we consider the evolution of directional width under a constant wind, with wind speed equal to $3c_p$ and $5c_p$, where $c_p$ is the phase speed of the initial spectral peak. The initial conditions, identical for all three models, are taken in the form of Donelan et al (1985) spectra for the corresponding wind speed. Third, we perform numerical simulations, with all three numerical approaches, of the evolution of wind waves observed in the Tehuantepec experiment (Romero & Melville, 2010) and compare the results with the observations.

The paper is organized as follows. Section 2 contains basic equations and brief description of the numerical algorithms and parameters. In section 3, results of the numerical simulations are discussed. Section 4 provides conclusions and a brief discussion.

# 2 Basic equations and numerics

## 2.1 The Zakharov equation and wave kinetic equations

Our starting point is the equation of motion in the form of the "four-wave" integrodifferential Zakharov equation originally derived for potential gravity waves at the surface of ideal incompressible fluid of infinite depth, with the accuracy up to $O(\varepsilon^3)$ (Zakharov , 1968; Krasitskii, 1994)

$$\mathrm{i}\frac{\partial b_0}{\partial t} = \omega_0 b_0 + \int T_{0123} b_1^* b_2 b_3 \delta_{0+1-2-3}\, \mathrm{d}\mathbf{k}_{123}\,, \tag{1}$$

where the wave field is expressed in terms of complex canonical variables $b(\mathbf{k})$ linked to the Fourier harmonics of the surface elevation $\zeta(\mathbf{k})$ and velocity potential at the surface $\psi(\mathbf{k})$ through an integral-power series:

$$b(\mathbf{k}) = \frac{1}{\sqrt{2}}\left\{\sqrt{\frac{\omega(\mathbf{k})}{k}}\zeta(\mathbf{k}) + \mathrm{i}\sqrt{\frac{k}{\omega(\mathbf{k})}}\psi(\mathbf{k})\right\} + O(\varepsilon)\,. \tag{2}$$

Compact notation is used, designating arguments by indices, e.g. $\delta_{0+1-2-3} = \delta(\mathbf{k}_0 + \mathbf{k}_1 - \mathbf{k}_2 - \mathbf{k}_3)$, $\mathrm{d}\mathbf{k}_{123} = \mathrm{d}\mathbf{k}_1\mathrm{d}\mathbf{k}_2\mathrm{d}\mathbf{k}_3$. The interaction coefficient $T_{0123}$ is given by an explicit but lengthy expression (e.g. Krasitskii, 1994).

Equation (1) is the basis for the derivation of the wave kinetic equation. Consider ensembles of random wave fields, assuming spatial homogeneity. Then the spectral density of wave action at wavevector $\mathbf{k}_0$ is the second-order correlator $n_0$,

$$\langle b_0^* b_1\rangle = n_0\delta_{0-1}\,.$$

By multiplying the Zakharov equation by $b_0^*$, upon ensemble averaging we get

$$\frac{\partial n_0}{\partial t} = 2\mathrm{Im}\int T_{0123}\langle b_0^* b_1^* b_2 b_3\rangle \delta_{0+1-2-3}\,\mathrm{d}\mathbf{k}_{123}\,. \tag{3}$$

In a similar way we can express time derivative of the fourth-order correlator in terms of the sixth-order one and so on. This infinite chain of equations can be truncated invoking the closure hypothesis (e.g. Zakharov *et al.*, 1992; Nazarenko, 2011). Since the statistics of a linear wave field is gaussian, the natural assumption is that the statistics of a weakly nonlinear field will be quasi-gaussian. Following Zakharov *et al.* (1992), we assume that the third-order correlator is zero. The fourth-order correlator can be always presented as

$$\langle b_0^* b_1^* b_2 b_3\rangle = [n_0 n_1(\delta_{0-2}\delta_{1-3} + \delta_{0-3}\delta_{1-2})] + J^{(1)}_{0123}\delta_{0+1-2-3},$$

where $J^{(1)}_{0123}$ is the irreducible part of the correlator (cumulant), which determines the evolution of $n_0$. To find the evolution of $J^{(1)}_{0123}$ we express it in terms of the sixth-order correlator, in which we retain just the dominant terms—the products of pair correlators

$$\left(\mathrm{i}\frac{\partial}{\partial t} + \Delta\omega\right) J^{(1)}_{0123} = -2T_{0123} f_{0123}, \tag{4}$$

where $\Delta\omega = \omega_0 + \omega_1 - \omega_2 - \omega_3$, $f_{0123} = n_2 n_3 (n_0 + n_1) - n_0 n_1 (n_2 + n_3)$. The derivation of the classical KE drops $\partial/\partial t$ from the equation for the cumulant $J^{(1)}_{0123}$, which leads to the approximate solution for large time in terms of generalised functions

$$J^{(1)}_{0123}(t) = -2T_{0123}\left[\frac{P}{\Delta\omega} + \mathrm{i}\pi\delta(\Delta\omega)\right] f_{0123}(t),$$

where $P$ is "principal value", $\delta$ is Dirac $\delta$-function. This leads to the KE

$$\frac{\partial n_0}{\partial t} = 4\pi \int T^2_{0123} f_{0123} \delta_{0+1-2-3} \delta(\omega_0 + \omega_1 - \omega_2 - \omega_3)\, \mathrm{d}\mathbf{k}_{123}, \tag{5}$$

The gKE is derived using the same statistical closure as the KE, but without the assumption of quasi-stationarity and the use of large time asymptotics. Instead, the equation for the cumulant $J^{(1)}_{0123}$ (4) is solved exactly (Annenkov & Shrira, 2006*a*)

$$J^{(1)}_{0123}(t) = -2\mathrm{i}T_{0123} \int_0^t \mathrm{e}^{-\mathrm{i}\Delta\omega(\tau - t)} f_{0123}(\tau)\, \mathrm{d}\tau + J^{(1)}_{0123}(0)\mathrm{e}^{\mathrm{i}\Delta\omega t}.$$

Then the resulting equation (gKE) has the form

$$\begin{aligned} \frac{\partial n_0}{\partial t} \;=\; & 4\mathrm{Re} \int \left\{ T^2_{0123} \left[ \int_0^t \mathrm{e}^{-\mathrm{i}\Delta\omega(\tau - t)} f_{0123}(\tau)\, \mathrm{d}\tau \right] \right. \\ & \left. -\frac{\mathrm{i}}{2} T_{0123} J^{(1)}_{0123}(0) \mathrm{e}^{\mathrm{i}\Delta\omega t} \right\} \delta_{0+1-2-3}\, \mathrm{d}\mathbf{k}_{123}\,. \end{aligned} \tag{6}$$

The gKE is nonlocal in time: evolution of the spectrum depends on the previous history of evolution, starting from the initial moment when the value of cumulant $J^{(1)}_{0123}(0)$ is prescribed as the initial condition. However, the gKE can be solved iteratively. On each time step, the value of $J^{(1)}_{0123}$ is computed as

$$J^{(1)}_{0123}(t) = -2\mathrm{i}T_{0123} \int_0^t \mathrm{e}^{-\mathrm{i}\Delta\omega(\tau - t)} f_{0123}(\tau)\, \mathrm{d}\tau + J^{(1)}_{0123}(0)\mathrm{e}^{\mathrm{i}\Delta\omega t} \tag{7}$$

and taken as the new initial condition, so that the 'internal' time integration is performed over one timestep only. Analytical results concerned with the gKE are summarised in Shrira & Annenkov (2013).

## 2.2 Numerics

In this study, we use three different algorithms for three different models: the classic KE (Hasselmann), the gKE, and our DNS algorithm based on the Zakharov equation (DNS-ZE). For the KE, we use the standard WRT code kindly provided by Gerbrant van Vledder. Two other algorithms are original.

Although the gKE at first glance looks much more complicated than the KE, and requires to take into account a large number of interactions, including those far from resonance, the

algorithm has a simpler structure and can be parallelized with nearly perfect scalability, thus efficiently utilizing the advantages of modern supercomputers. The nonlocality in time can be treated by accumulating all the previous history in the value of the cumulant $J^{(1)}_{0123}$, which is taken as the initial condition at each time step. We employ the standard Runge-Kutta-Fehlberg time-stepping algorithm with automatic step choice. Details of the algorithm can be found in Annenkov & Shrira (2016).

The DNS algorithm is based on the efficient algorithm for the simulation of the evolution of discrete wave systems, employing the integrodifferential Zakharov equation (Annenkov and Shrira, 2001). In that study, a wave field $b(\mathbf{k}, t)$ was considered as an ensemble of discrete harmonics of the form

$$b(\mathbf{k}, t) = \sum_{j=1}^{N} b_j(\mathbf{k}_j, t). \tag{8}$$

The DNS-ZE algorithm is essentially an application of the original algorithm of Annenkov and Shrira (2001) to the evolution of continuous random wave fields. It is based on the idea of coarse-graining of a continuous wave field, retaining its fundamental properties of nonlinear interactions. The coarse-graining represents a wave field by a grid consisting of wave packets, coupled through exact and approximate resonant interactions. The resulting system of discrete dynamical equations is again solved by Runge-Kutta-Fehlberg time-stepping scheme. The DNS-ZE algorithm was described in detail by Annenkov & Shrira (2013, 2018).

For all computations in this work, we use non-regular grids with $N_\omega$ logarithmically spaced points in the range $\omega_p/2 \le \omega \le 3\omega_p$ and $N_\theta$ uniformly spaced angles. The KE is simulated in the full circle of the angles $\theta$, since this is preferable for the existing WRT code. The gKE and DNS-ZE algorithms can work in any sector of $\theta$, and a sector $-7\pi/9 \le \theta \le 7\pi/9$, sufficiently wide for the purposes of the present study, was used. The frequency resolution was chosen as $N_\omega = 160$ for the DNS-ZE, and $N_\omega = 100$ for both kinetic equations. Angular resolution was $N_\theta = 70$ within $-7\pi/9 \le \theta \le 7\pi/9$ for the DNS, $N_\theta = 30$ within the same sector for the gKE, and $N_\theta = 50$ in full circle for the KE. In some computations which involved initially narrow spectra (§ 3.1 below), angular resolution for both kinetic equations was refined, and results were verified to be non-dependent on any further refinement.

# 3 Results

Here we consider results of simulations for several different cases of spectral evolution with or without wind forcing, focussing on the evolution of directional spreading. As a measure of directional spreading, we use the second moment of the normalized angular distribution function $D(k, \theta)$ (Hwang *et al.*, 2000, eg)

$$\theta_2(k) = \left( \int_0^{\pi/2} \theta^2 D(k, \theta)\, \mathrm{d}\theta \right)^{1/2} \left( \int_0^{\pi/2} D(k, \theta)\, \mathrm{d}\theta \right)^{-1/2}, \tag{9}$$

Often, directional spreading is characterized by the *mean directional spread* $\theta_m$, defined as the average of $\theta_2$ over $k$ (Xiao *et al.*, 2013; Annenkov & Shrira, 2018). Being a scale averaged

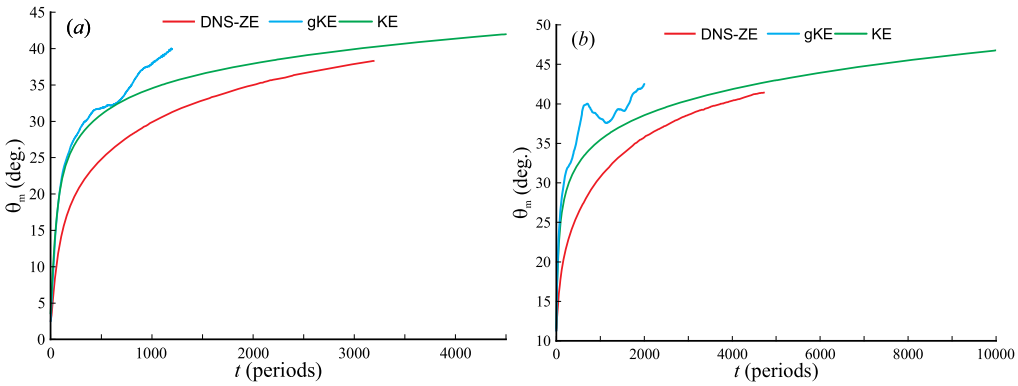


Figure 1: Evolution of averaged second moment of directional distribution $\theta_m$ without wind forcing. Initial conditions are JONSWAP spectra with $\gamma = 6$ and narrow directional spreading, corresponding to (a) N=850 (b) N=24 in the $\cos^N$ directional model.

characteristics of the angular spectrum, $\theta_m$ provides only the most basic information about its width. Since $D(k, \theta)$, angular distributions at all wavenumbers play equal role, regardless of the spectral amplitude, diminishing the relative contribution from the spectral peak. In order to understand the evolution of the angular distributions at key parts of the spectrum, at the spectral peak, slope and front separately, along with $\theta_m$ we consider the evolution of $theta_2$ for at selected specific values of $k$, relative to the spectral peak $k_p$ ($0.5k_p$, $k_p$, $2k_p$ and $3k_p$).

In the rest of this section, we consider three spectral evolution scenarios: evolution of initially narrow (both in frequency and angle) spectra without wind forcing, evolution of directionally wide spectra under constant wind, and simulation of a realistic observation-based wind wave evolution, with comparison with the experimental data.

## 3.1 Evolution of initially narrow spectra without wind

The laboratory experiment by Onorato *et al.* (2009), who studied short-term (about 30 wavelength) evolution of wave spectra having initially JONSWAP form and different directional distributions provided inspiration for a few studies that aimed at modelling the same evolution numerically. Xiao *et al.* (2013) performed numerical modelling using high-order spectral method with high resolution, taking as initial conditions the spectra generated mechanically in the experiment and simulating their evolution for about 150 wave periods. Two of these spectra had JONSWAP form with peakedness $\gamma = 6$, significant wave height $H_s = 0.08$ m, the peak period $T_p = 1$ s, and different directional distributions $D(\theta)$, given by cosine square

$$D(\theta) = \begin{cases} \dfrac{2}{\Theta} \cos^2\left(\dfrac{\pi\theta}{\Theta}\right) & \text{for} \quad |\theta| \le \Theta/2 \\ 0 & \text{for} \quad |\theta| > \Theta/2 \end{cases} \tag{10}$$

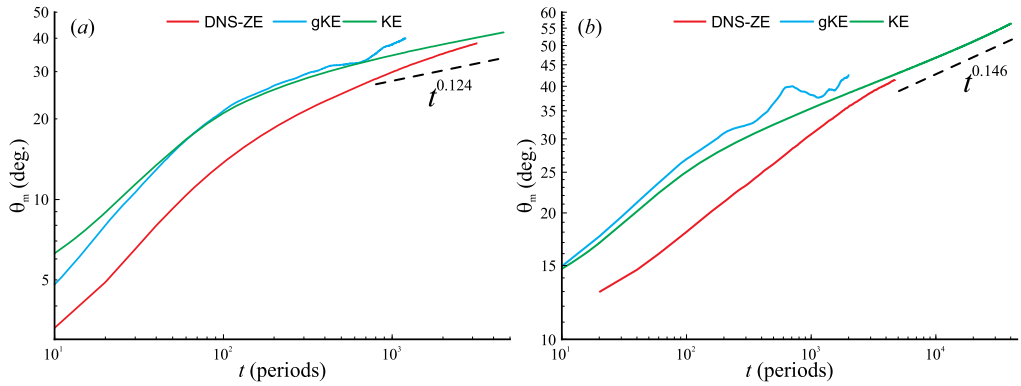


Figure 2: As in figure 1, in logarithmic coordinates, and power fits for the KE results for large time

where $\Theta$ is the directional spreading width in radians. The first spectrum was very narrow in angle with $\Theta = \pi/15$, approximately corresponding to $N = 840$ in the $\cos^N$ directional model. The second spectrum was wider, with $\Theta = \pi/2.9$, corresponding to $N = 24$. This angular width can be considered as typical width of swell.

Recently, Annenkov & Shrira (2018) performed numerical experiments with the same initial conditions, using three numerical models (the KE, the gKE, and the DNS-ZE), focussing mostly on one-dimensional spectral evolution. Using the advantages of the DNS-ZE, these simulations were performed for thousands of wave periods. The validation of the DNS-ZE algorithm was provided by quantitative comparisons with the results of short-term DNS simulations by Xiao *et al.* (2013)) and tank observations by Onorato *et al.* (2009). Long-term simulations allowed Annenkov & Shrira (2018) to reveal fundamental differences between the predictions of the kinetic equations and DNS. These differences were attributed to the role of the statistical closure.

One of these differences was in the rate of directional spreading at the initial stage of the evolution, which was found to be much faster for the kinetic equations than for the DNS-ZE, although the latter was in close agreement with the results by Xiao *et al.* (2013). The long-term angular width evolution appeared to tend to the same limiting angle for all three models. However, since the focus of Annenkov & Shrira (2018) was on one-dimensional evolution, all computations were performed for a relatively narrow range of angles $-4\pi/9 \le \theta \le 4\pi/9$, identical for all models to facilitate the comparison between them.

For this work, all simulations involving the KE have been recomputed in the full circle, with the base resolution of $N_\theta = 50$, $-\pi \le \theta \le \pi$. For the narrow $N = 840$ case, this angular resolution was found to be insuffient at the initial stage of the evolution, so $N_\theta$ was increased to 130. Simulations with the gKE and the DNS-ZE were found to have sufficient resolution and to be unaffected by the angular limits for the time span of the simulations. In this work, these simulations are used unchanged.

Figure 1a,b shows the long-term evolution of the averaged second moment $\theta_m$ for both initial

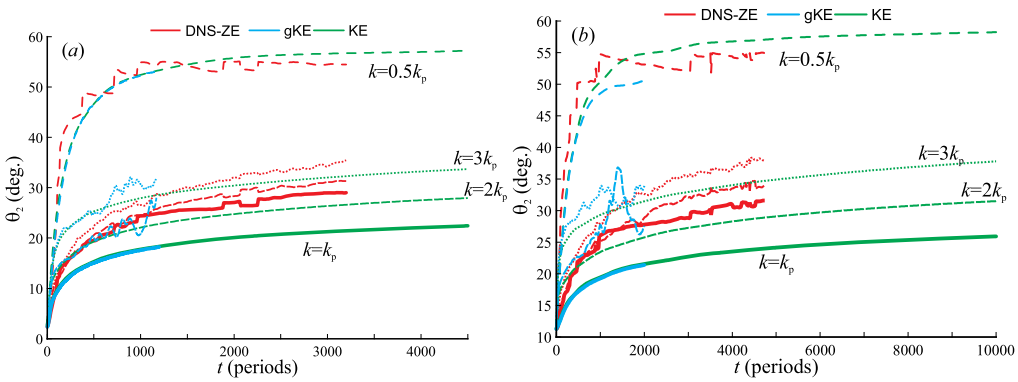


Figure 3: Evolution of second moment of directional distribution $\theta_2(k)$ at wavenumbers $k = k_p$, $0.5k_p$, $2k_p$ and $3k_p$, for two initially JONSWAP spectra with $\gamma = 6$ and narrow directional spreading, corresponding to (a) N=850 (b) N=24 in the $\cos^N$ directional model

spectra, obtained with the KE, the gKE and the DNS-ZE. Computations for different models were performed for different times, due to the numerical instability of the gKE in the high frequencies, which is particularly effective without wind forcing (Annenkov & Shrira, 2018), and high computational cost of the DNS-ZE simulations, which involved averaging over 100 realizations. Case (b), with wider initial angular spectrum, was traced for larger time to get a more complete picture of long-term behaviour. In the short term, both kinetic equations give nearly identical results and demonstrate much faster angular expansion than the DNS-ZE. In the long term, the least-squares fit for the KE shows slow powerlike growth of $\theta_m$, and all models appear to tend to it (figure 2a,b). The exponents for the powerlike growth are slightly different for the two initial spectra, apparently due to a large difference in angular resolution. While $\theta_m$ is an averaged characteristic, a more comprehensive picture of the directional spreading can be obtained from the evolution of the second moment $\theta_2(k,t)$ at different $k$. This evolution, for a few values of $k$ relative to the spectral peak $k_p$, is shown in figure 3a,b. All three models nearly coincide for $\theta 2(0.5k_p, t)$, but at the spectral peak and for higher $k$ the DNS-ZE demonstrates a larger angular width at large times than the kinetic equations, although with close rates of growth. However, the gradient of the angular width with respect to wavenumber is higher for the KE, so that the difference in the averaged $\theta_m$ becomes small at large times due to the role of the highest wavenumbers.

Badulin & Zakharov (2017), having performed the long-term simulations with the KE of the evolution of swell of different initial angular width, found that the angular width at the spectral peak at large times tends to a certain universal value, although they provided only a qualitative demonstration of the approach to this limit. Our simulation with the KE shows that the growth at the spectral peak continues even for large times ($\gg 10^4$ periods), although it becomes very slow.

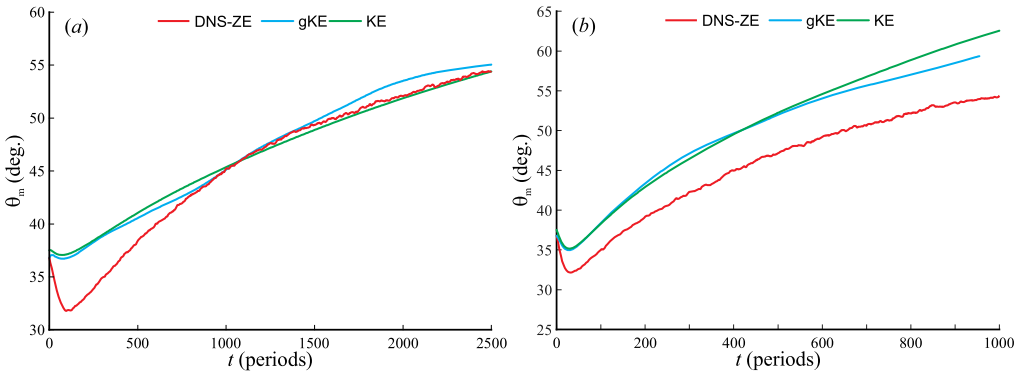


Figure 4: Evolution of averaged second moment of directional distribution $\theta_m$ for wind waves, with wund speed (a) $U/c_p = 3$ (b) $U/c_p = 5$, where $c_p$ is the phase speed of the initial spectral peak

## 3.2 Evolution of wind wave spectra with constant wind forcing

Here, we consider the evolution of wind wave spectra under the action of constant wind, for two different wind speeds, corresponding to either moderate or strong wind. Initial conditions, including the initial directional distribution, are specified in the form of the empirical spectra by Donelan et al (1985) for $U/c_p = 3$ (moderate wind) or 5 (strong wind), where $U$ is the wind speed and $c_p$ is the initial phase speed of the spectral peak. The subsequent wind forcing, for the same wind speed, modelled according to Hsiao and Shemdin (1983), applied to frequencies $\omega \leq 2.5\omega_p$, where $\omega_p$ is the initial spectral peak frequency. Dissipation is applied to $\omega > 2.8\omega_p$. Simulations are performed with the same frequency discretizations as before. The angular discretization involves 50 uniformly spaced angles for the KE, 30 angles within $-7\pi/9 \leq \theta \leq 7\pi/9$ for the gKE and 70 angles within the same sector for the DNS-ZE. The DNS-ZE algorithm includes a simple parameterization of wave breaking: in all realizations all harmonics within the forcing domain are subjected to strong dissipation instead of forcing if they exceed a certain level of nonlinearity. Only a small number of harmonics is affected by this breaking parameterization (typically, 1–10 for moderate wind and 10–20 for strong wind, out of the total number of 11431). Averaging for the DNS-ZE is over 20 realizations.

Figure 4 shows the evolution of the averaged second moment $\theta_m$ for both cases. Since initial spectra are already directionally wide, the change of angular width during evolution is much smaller than in the previous section. All spectra initially adapt to the constant wind forcing over the first few hundred periods, after which the evolution of $\theta_m$ is very similar for all models, showing a gradual increase of angular width. For strong wind, there is a relatively small systematic difference between the DNS-ZE and both kinetic equations, which give almost identical results between themselves. This difference is likely to be due to a different shape of directional distribution in the case of the DNS-ZE, which requires a special study.

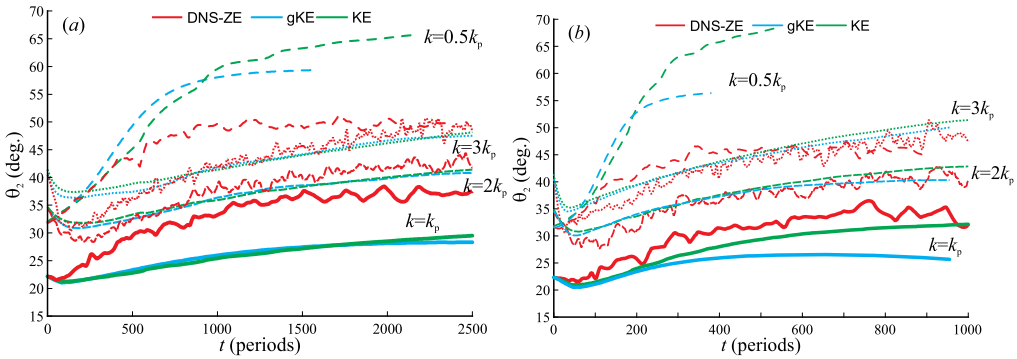


Figure 5: Evolution of second moment of directional distribution $\theta_2(k)$ at wavenumbers $k = k_p$, $0.5k_p$, $2k_p$ and $3k_p$ for wind waves, with wind speed (a) $U/c_p = 3$ (b) $U/c_p = 5$, where $c_p$ is the phase speed of the initial spectral peak

The details of the angular distribution, as shown in figure 5, reveal a close agreement for angular width at higher wavenumbers between the three models, but a large discrepancy for large scales, where the DNS-ZE gives a considerably narrower angular distribution. For small scales, the angular width continues to increase at large times, while at the spectral peak it saturates.

### 3.3 Evolution of wind wave spectra in natural conditions

In the Tehuantepec experiment, Romero & Melville (2010) performed high quality airborne measurements of two-dimensional wind wave spectra with simultaneous measurements of wind, over a few hundred kilometers of fetch. Here we model one particular example of this evolution (corresponding to research flight 10 of the experiment) numerically, taking as the initial condition the two-dimensional spectrum measured at fetch 100 km offshore, where wind waves start dominating over opposing swell. During the evolution, wind is gradually weakening and turning clockwise by about 40 degrees, the wind data being input into the numerical models using, as before, the paramaterization by Hsiao and Shemdin (1983). The same numerical grid as in the previous section was used, the initial condition and wind data renormalized accordingly. Averaging for the DNS-ZE was performed over 30 realizations. The opposing swell and its effect on wind waves are not modelled.

Figure 6 shows the evolution of $\theta_m$ for three numerical models, and comparison with $\theta_m$ obtained from the data. It demonstrates a rough consistency of all the models with the observations. Figure 7, which details the evolution of the angular width for different wavenumbers, reveals a complex picture. For long waves, the angular width is identical for all the models, but quite different from the data, apparently due to the presence of swell. For the spectral peak and shorter waves, the DNS-ZE shows good agreement with the data, demonstrating slow growth of angular width over time at the spectral peak (in contrast to nearly constant width shown by the

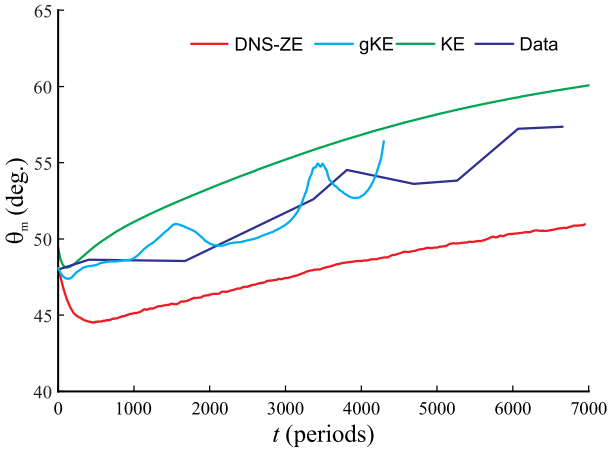


Figure 6: Evolution of averaged second moment of directional distribution $\theta_m$ for wind waves in the Tehuantepec experiment (Romero & Melville, 2010), data and numerical modelling

kinetic equations) and weak dependence of angular width on wavenumber.

# 4 Concluding remarks

Better description of the evolution of the directional spectra is key for probing the adequacy of our present understanding of the underpinning physical mechanisms. In this work, we examined a few representative examples of the evolution of directional wave spectra (with and without wind forcing) obtained numerically using simulations with three different models, based on different sets of assumptions. By comparing the results of simulations with different models and against the Tehuantepec observations we have got important insights into the ability of existing numerical tools to capture the angular evolution of wave spectra.

As a quantitative characteristics of wave field directionality we confined our attention to the directional width, as given by the second moment of the angular distribution function, calculated at a few "characteristic" wavenumbers relative to the spectral peak, or averaged over all wavenumbers. For the case of swell, initially narrow in angle, we have found that although the kinetic equations, compared with the DNS-ZE, considerably overestimate the rate of the initial angular broadening, the integrated angular width at large time approaches the same powerlike asymptote, corresponding to slow broadening with time. However, the DNS-ZE shows a weaker dependence of the angular width on wavenumber. Within all models, the angular width of the spectral peak continues to grow slowly even for large time. For constant wind forcing, the models agree well on the spectral width of the spectral tail, but show large discrepancies for small wavenumbers. For the case of the Tehuantepec experiment data, the DNS-ZE is consistent with the data, demonstrating slow growth of angular width over time at the spectral peak, in contrast

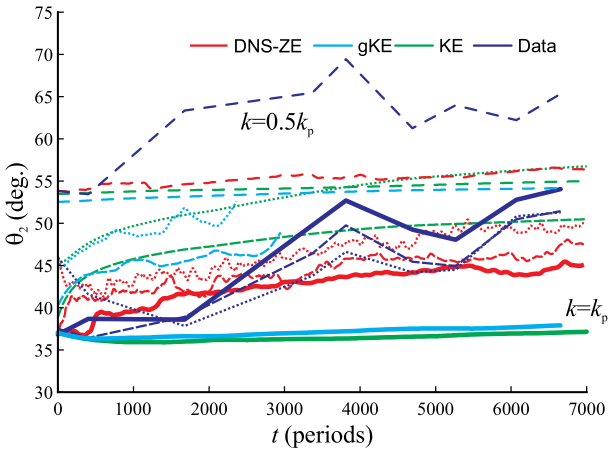


Figure 7: Evolution of second moment of directional distribution $\theta_2(k)$ at wavenumbers $k = k_p$, $0.5k_p$, $2k_p$ and $3k_p$ for wind waves in the Tehuantepec experiment, data and numerical modelling

to nearly constant width shown by the kinetic equations, and weak dependence of angular width on wavenumber. The overall conclusion is that the modelling based upon the Hasselmann kinetic equation or gKE does not capture well the evolution of the angular width, DNS-ZE does a much better job in this respect.

The results presented have important, although not necessarily short term, implications. The knowledge of the directional distribution of water waves is essential for various practical applications. Accurate measurements of two-dimensional spectra are rare, and most of the existing understanding of directional properties comes from modelling, which is almost exclusively based on the Hasselmann kinetic equation. Understanding the role of the assumptions underlying the KE is necessary for improving wave prediction models. From the theoretical perspective, revealing the discrepancies between the kinetic equations and the DNS helps understand the role of the statistical closure in kinetic models, which is important both within and beyond the water wave context.

We are grateful to G. van Vledder for providing his WRT code, and to L. Romero and W. K. Melville for the access to Tehuantepec experiment data. The work was supported by UK NERC grant NE/I01229X/1. Computations were performed on the CUDA High Performance Computing cluster at Keele University and on the ECMWF Supercomputing facility within the Special Project SPGBSHRI.

## References

Annenkov, S. Y. and Shrira, V. I. 2001 Numerical modelling of water waves evolution based on the Zakharov equation. *J. Fluid Mech.* **449**, 341–371.

Annenkov, S. Y. & Shrira, V. I. 2006 Role of non-resonant interactions in the evolution of nonlinear random water wave fields. *J. Fluid Mech.* **561**, 181–207.

Annenkov, S. Y. & Shrira, V. I. 2009 "Fast" nonlinear evolution in wave turbulence. *Phys. Rev. Lett.* **102**, 024502.

Annenkov, S. Y. & Shrira, V. I. 2011 Evolution of wave turbulence under "gusty" forcing. *Phys. Rev. Lett.* **107**, 114502.

Annenkov, S. Y. & Shrira, V. I. 2013 Large-time evolution of statistical moments of a wind wave field. *J. Fluid Mech.* **726**, 517–546.

Annenkov, S. Y. & Shrira, V. I. 2016. Modelling transient sea states with the generalised kinetic equation. In: *Rogue and Shock Waves in Nonlinear Dispersive Media*. Springer, pp. 159–178.

Annenkov, S. Y. & Shrira, V. I. 2018 Spectral evolution of weakly nonlinear random waves: kinetic description versus direct numerical simulations. *J. Fluid Mech.* **844**, 766–795.

Badulin, S. I. & Zakharov, V. E. 2017 Ocean swell within the kinetic equation for water waves. *Nonlin. Proc. Geophys.* **24**, 237–253.

Donelan, M. A., J. Hamilton & Hui, W. H. 1985 Directional spectra of wind-generated waves. *Phil. Trans. R. Soc. London* **A315**, 509–562.

Ewans, K. C. 1998 Observations of the directional spectrum of fetch-limited waves. *J. Phys. Oceanogr.***28**, 495–512.

Goda, Y. 2010 *Random seas and design of maritime structures.* World Scientific.

Holthuisen, L. H. *Waves in oceanic and coastal waters.* Cambridge University Press.

Hwang, P. A., Wang, D. W., Walsh, E. J., Krabill, W. B. & Swift, R. N. 2000 Airborne measurements of the wavenumber spectra of ocean surface waves. Part II: Directional distribution. *J. Phys. Oceanogr.* **30**, 2768–2787.

Krasitskii, V. P. 1994 On reduced Hamiltonian equations in the nonlinear theory of water surface waves. *J. Fluid Mech.* **272**, 1–20.

Mitsuyasu, H., Tasai, F., Suhara, T., Mizuno, S., Ohkusu, M., Honda, T. & Rikiishi, K. 1975 Observations of the directional spectrum of ocean WavesUsing a cloverleaf buoy. *J. Phys. Oceanogr.* **5**, 750–760.

Nazarenko, S. V. 2011 *Wave Turbulence*. Springer.

Newell, A. C. & Rumpf, B. 2013 Wave turbulence: A story far from over. In: *Advances in Wave Turbulence, World Scientific Series on Nonlinear Science, 83*, pp. 1–51.

Onorato, M., Cavaleri, L., Fouques, S., Gramstad, O., Janssen, P.A.E.M., Monbaliu, J., Osborne, A.R., Pakozdi, C., Serio, M., Stansberg, C.T. & Toffoli, A. 2009 Statistical properties of mechanically generated surface gravity waves: a laboratory experiment in a three-dimensional wave basin. *J. Fluid Mech.* **627**, 235–257.

Hsiao, S. V. & Shemdin, O. H. 1983 Measurements of wind velocity and pressure with a wave follower during MARSEN. *J. Geophys. Res.* **88**, 9841–9849.

Romero, L. & Melville, W. K. 2010 Airborne observations of fetch-limited waves in the Gulf of Tehuantepec. *J. Phys. Oceanogr.* **40**, 441–465.

Shrira, V. I. & Annenkov, S. Y. 2013 Towards a new picture of wave turbulence. In: *Advances in Wave Turbulence, World Scientific Series on Nonlinear Science, 83*, pp. 239–281.

Tanaka, M. 2001 Verification of Hasselmann's energy transfer among surface gravity waves by direct numerical simulations of primitive equations. *J. Fluid Mech.* **444**, 199–221.

Toffoli, A., Gramstad, O., Trulsen, K., Monbaliu, J., Bitner-Gregersen, E. & Onorato, M. 2010 Evolution of weakly nonlinear random directional waves: laboratory experiments and numerical simulations. *J. Fluid Mech.* **664**, 313–336.

Xiao, W., Liu, Y., Wu, G. & Yue, D. K. 2013 Rogue wave occurrence and dynamics by direct simulations of nonlinear wave-field evolution. *J. Fluid Mech.* **720**, 357–392.

Young, I. R., Verhagen, L. A. & Banner, M. L. 1995 A note on the bimodal directional spreading of fetch-limited wind waves. *J. Geophys. Res.* **100**, 773–778.

Zakharov, V. E. 1968 Stability of periodic waves of finite amplitude on the surface of a deep fluid. *J. Appl. Mech. Tech. Phys.* (USSR) **9**, 86–94.

Zakharov, V. E., L'vov, V. S. & Falkovich, G. 1992 *Kolmogorov Spectra of Turbulence I: Wave Turbulence.* Springer.